

A novel DEM reconstruction strategy based on multi-frequency InSAR in highly sloped terrain

Tao ZENG, Tiandong LIU, Zegang DING*, Qi ZHANG, Zhen WANG & Teng LONG

*Beijing Key Laboratory of Embedded Real-time Information Processing Technology,
Beijing Institute of Technology, Beijing 100081, China*

Received July 15, 2016; accepted October 12, 2016; published online March 10, 2017

Citation Zeng T, Liu T D, Ding Z G, et al. A novel DEM reconstruction strategy based on multi-frequency InSAR in highly sloped terrain. *Sci China Inf Sci*, 2017, 60(8): 088301, doi: 10.1007/s11432-016-0085-4

Interferometric Synthetic Aperture Radar (InSAR) has been proposed as a technique for the reconstruction of the Digital Elevation Model (DEM), which is widely used in global terrain mapping mission [1]. The DEM reconstruction methods of InSAR technique are usually based on the so-called phase unwrapping (PU) operation. In highly sloped terrain, the interferometric phase gradients (IPG) of the adjacent pixels are more than π . Therefore, the traditional PU methods cannot correctly obtain the absolute interferometric phase (IP) [2]. Several methods based on multi-frequency InSAR (MF-InSAR), such as the maximum likelihood (ML) method, maximum a posteriori (MAP) method, and so on, have been widely studied. The ML method can quickly obtain the estimation of target heights [3]. However, its performance largely depends on the number of interferograms, and the estimation results also can be easily influenced by the phase noise. Compared to the ML method, the MAP method can reduce the number of interferograms, but it suffers from some other limitations, such as the computational time [4].

This article proposes a novel DEM reconstruction strategy based on MF-InSAR. In the InSAR

system, the probability density function (PDF) of the IPG $f_{\Delta\varphi}$ can be calculated in [5]. In the MF-InSAR system, the work frequencies satisfy $f_1 \leq f_2 \leq \dots \leq f_l$. By using the highest work frequency as the reference frequency, we can convert the IPG of other work frequencies, and the joint PDF of the column IPG $f_{\text{MF-InSAR}}$ in MF-InSAR can be described as (1), the PDF of row IPG can be described as the same method.

$$f_{\text{MF-InSAR}}[\Delta_{\text{col}}\Phi; \Delta_{\text{col}}\phi_l] = \prod_{k=1}^l \left(\frac{f_k}{f_l}\right) \cdot f_{\Delta\varphi} \left[\left(\frac{f_l}{f_k}\right) \cdot \Delta_{\text{col}}\varphi_k; \Delta_{\text{col}}\phi_l \right], \quad (1)$$

where $\Delta_{\text{col}}\Phi = [(\frac{f_l}{f_1}) \cdot \Delta_{\text{col}}\varphi_1, \dots, (\frac{f_l}{f_k}) \cdot \Delta_{\text{col}}\varphi_k]$, $\Delta_{\text{col}}\varphi_k$ stands for the column IPG of the k th work frequency, $\Delta_{\text{col}}\phi_l$ stands for the column IPG of the corresponding nominal value of the reference frequency.

However, the estimation results based on (1) are vulnerable to phase noise [3]. To solve this problem, a local adjacent pixel set (LAPS) of the IPG is proposed to improve the robust of this algorithm. A 3×3 LAPS around the center point P is $\mathbf{S} = \{\mathbf{S}_1, \mathbf{S}_2, \mathbf{S}_3, \mathbf{S}_4, \mathbf{S}_5, \mathbf{S}_6, \mathbf{S}_7, \mathbf{S}_8\}^T$. Due to the influence of the phase noise, the reconstruction

* Corresponding author (email: z.ding@bit.edu.com)

The authors declare that they have no conflict of interest.

accuracy of the IPG will be low if the IPG selected rely on the peak value. Assuming that there are N peak values in the searching interval, which are all arranged from the largest to smallest. Then the IPG can be selected from the first n ($n \leq N$) peak values as the estimation vector of point P

$$\Delta_{\text{col}}\varphi_P = \{\Delta_{\text{col}}\varphi_P^1, \dots, \Delta_{\text{col}}\varphi_P^n\}^T, \quad (2)$$

where $\Delta_{\text{col}}\varphi_P$ stands for the IPG estimation vector of point P , $\Delta_{\text{col}}\varphi_P^i$, $i = 1, \dots, n$ stand for the IPG of point P selected by the first n th peak.

Same as point P , the IPG estimation vector of other pixels in the LAPS can be described as

$$\begin{aligned} \mathbf{S}_i &= \Delta_{\text{col}}\varphi_{\mathbf{S}_i} \\ &= \{\Delta_{\text{col}}\varphi_{\mathbf{S}_i}^1, \dots, \Delta_{\text{col}}\varphi_{\mathbf{S}_i}^n\}^T, \quad i = 1, \dots, 8, \end{aligned} \quad (3)$$

where $\Delta_{\text{col}}\varphi_{\mathbf{S}_i}$ stands for the estimation vector of adjacent pixel \mathbf{S}_i and $\Delta_{\text{col}}\varphi_{\mathbf{S}_i}^n$ stands for the IPG corresponding to the n th maximum value of the adjacent pixel \mathbf{S}_i which is estimated by (1).

Then, we can improve the accuracy of the IPG by minimizing the difference of the IPG in the LAPS

$$\begin{aligned} \Delta_{\text{col}}\varphi_{\text{A-ML}}(P) &= \min_{n, \Delta_1\varphi_P^n} \sum_{\mathbf{S}_i} \|\Delta_{\text{col}}\varphi_P^n - \Delta_{\text{col}}\varphi_{\mathbf{S}_i}^n\|^2 \\ \text{s.t. } \Delta_{\text{col}}\varphi_P^n &\in \Delta_{\text{col}}\varphi_P \text{ and } \Delta_{\text{col}}\varphi_{\mathbf{S}_i}^n \in \mathbf{S}_i, \end{aligned} \quad (4)$$

where $\Delta_{\text{col}}\varphi_{\text{A-ML}}(P)$ stands for the improved value of the IPG based on LAPS.

After calculating the IPG of point P through (4), we can get the reconstruction column IPG of point P from (5),

$$\begin{aligned} \Delta_{\text{col}}\varphi_{\text{new}}(P) &= \Delta_{\text{col}}\varphi(P) \\ &+ 2\pi \cdot \text{round}\{[\Delta_1\varphi_{\text{A-ML}}(P) - \Delta_1\varphi(P)]/2\pi\}, \end{aligned} \quad (5)$$

where $\Delta_{\text{col}}\varphi_{\text{new}}(P)$ stands for the new column IPG value of point P reconstructed by LAPS, $\Delta_{\text{col}}\varphi(P)$ stands for the column IPG value of point P only calculated by (1), $\Delta_{\text{col}}\varphi(P)$ stands for the column IPG of point P which can be calculated by the wrapped IP directly, and $\text{round}(\cdot)$ stands for the rule of round off.

Finally, by using the the branch-cut phase unwrapping method [6], the absolute IP of the highly sloped terrain can be obtained from the reconstruction IPG results.

According to the method above, the PU method based on MF-InSAR can obtain the absolute IP in the highly sloped terrain, but when the phase isolated regions exist in the interferogram, the empty-holes will be appeared in the PU results and the DEM reconstruction results. Taking into account the ML method based on MF-InSAR can achieve

the elevation reconstruction of any terrain without the PU operation [3], so we can use the elevation results reconstructed by the ML method as a reference height value to compensate the elevation results reconstructed by the PU method based on MF-InSAR in the isolated regions. Firstly, the binary matrix of the branch-cuts is generated. Then, the phase isolated regions surrounded by the residuals are marked. After that, the region growing method is used to fill the isolated regions [7]. Finally, the ML method based on MF-InSAR is applied to correct the ambiguity numbers of the isolated regions, and then the elevation values of the isolated regions can be modified. The steps of this process can be described as follows:

Step 1: The MF-InSAR PU method mentioned above is carried out in the whole scene and the DEM reconstruction result is $h_{\text{A-ML}}$. Meanwhile, the binary matrix of the branch-cuts $\mathbf{T}_{\text{Branch-cuts}}$ is generated during the PU process;

Step 2: The ML method based on MF-InSAR is carried out to obtain the DEM reconstruction of the whole scene [3]. The result is h_{ML} ;

Step 3: According to the results above, combining with the IP of the reference frequency φ_l , the ambiguity number of the whole scene can be calculated by

$$n_1 = \left[\frac{h_{\text{ML}} \cdot 2\pi}{h_{\text{amb}}^l} - \varphi_l \right] / 2\pi, \quad (6)$$

$$n_2 = \left[\frac{h_{\text{A-ML}} \cdot 2\pi}{h_{\text{amb}}^l} - \varphi_l \right] / 2\pi, \quad (7)$$

where h_{amb}^l is the height ambiguity of the reference frequency.

Step 4: The region growing method is used to expand the isolated regions in the binary matrix of the branch-cuts [7], and the new binary matrix $\mathbf{T}_{\text{Branch-cuts}}^{\text{new}}$ is generated. After that, the local ambiguity number deviation of the isolated regions can be calculated by

$$n_{\text{bias}} = \frac{\sum_{i,j \in A} \{n_1(i,j) - n_2(i,j)\}}{A}, \quad (8)$$

where A represents the total number of the pixels in the isolated regions.

Step 5: Finally, the elevation values of the isolated regions are corrected by the local ambiguity number deviation, and the DEM reconstruction of the whole scene can be generated by

$$h_{\text{new}} = h_{\text{A-ML}} + n_{\text{bias}} \cdot h_{\text{amb}}^l \cdot \mathbf{T}_{\text{Branch-cuts}}^{\text{new}}. \quad (9)$$

Figure 1 shows the computer simulation results based on the real DEM data. In this simulation, the work frequencies are C-band (5.4 GHz) and X-band (9.6 GHz), the ambiguity height of two frequencies are 54.37 m and 30.41 m, respectively.

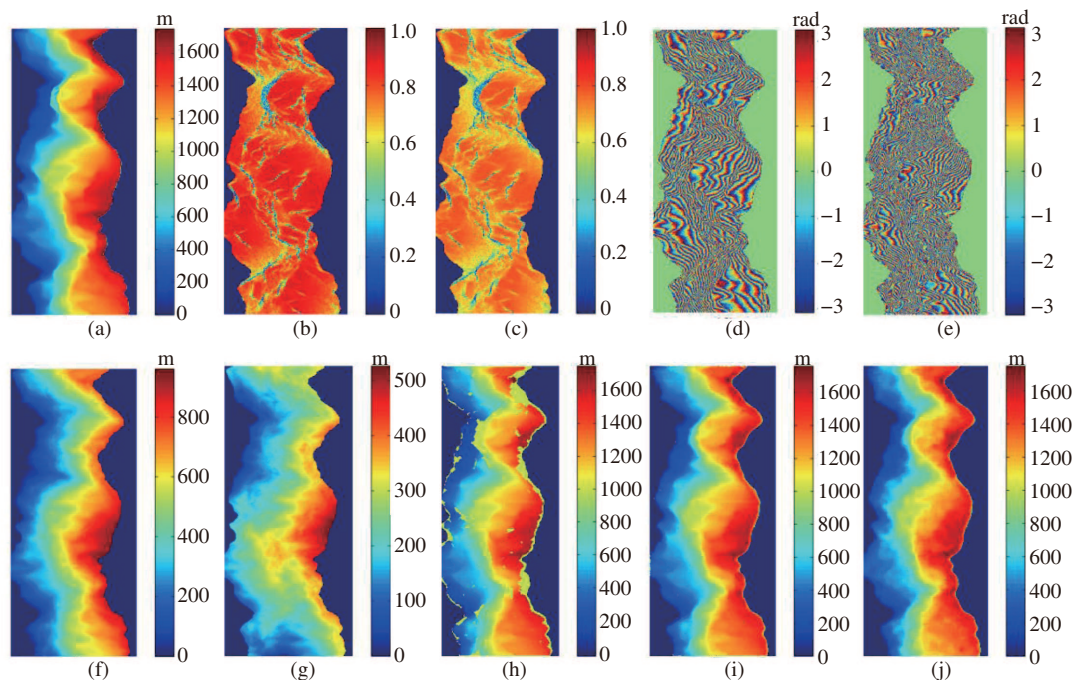


Figure 1 Computer simulation. (a) Original DEM; (b) correlation map of C-band; (c) correlation map of X-band; (d) interferogram of C-band; (e) interferogram of X-band; (f) DEM reconstruction by InSAR of C-band; (g) DEM reconstruction by InSAR of X-band; (h) DEM reconstruction by proposed method before isolated regions corrected; (i) DEM reconstruction by proposed method after isolated regions corrected; (j) DEM reconstruction by LPPE method.

Figure 1(a) stands for the real DEM data. Figure 1 (b) and (c) stand for the correlation maps of C-band and X-band, respectively. Figure 1 (d) and (e) stand for the interferograms of C-band and X-band, respectively. Figure 1 (f) and (g) stand for the DEM reconstructions by traditional InSAR of C-band and X-band, respectively. Figure 1 (h) and (i) stand for the DEM reconstructions by proposed method before and after isolated regions corrected, respectively. Figure 1(j) stands for the DEM reconstruction by local plane parameters estimation (LPPE) method proposed in [3]. The normalized reconstruction square errors of Figure 1 (f), (g), (i) and (j) are 5.4×10^{-1} , 9.8×10^{-1} , 1.1×10^{-3} and 1.6×10^{-3} , respectively. The operation times of Figure 1 (i) and (j) are 96.78 s and 821.65 s, respectively.

In this letter, a novel DEM reconstruction strategy based on MF-InSAR is proposed for the DEM reconstruction in highly sloped terrain. Firstly, the ML function of the IPG based on MF-InSAR is derived to obtain the ML estimation results of the IPG. Then, the LAPS is proposed to improve the estimation accuracy of the IPG. The reconstruction results of the IPG can be used to support the traditional PU method to realize the PU operation and DEM reconstruction in highly sloped terrain. Finally, the region growing algorithm and the the

ML method are used to correct the elevation of the isolated regions. The experiment based on real DEM data is demonstrated to verify the validity of this method.

Acknowledgements This work was supported by National Natural Science Foundation of China (Grant Nos. 61370017, 61032009, 61120106004).

References

- Bamler R, Hartl P. Synthetic aperture radar interferometry. *Inverse Probl*, 1998, 14: R1–R54
- Itoh K. Analysis of the phase unwrapping problem. *Appl Opt*, 1982, 21: 2470
- Baselice F, Budillo A, Ferraioli G, et al. Multibaseline SAR interferometry from complex data. *IEEE J-STARS*, 2014, 7: 2911–2918
- Hong F, Tang J W, Lu P P. Multichannel DEM reconstruction method based on Markov random fields for bistatic SAR. *Sci China Inf Sci*, 2015, 58: 062302
- Michael S, Johannes L S, Uwe S. Adaptive covariance matrix estimation for multi-baseline InSAR data stacks. *IEEE Trans Geosci Remote Sens*, 2014, 52: 6807–6817
- Liu H T, Xing M D, Bao Z. A cluster-analysis-based noise-robust phase-unwrapping algorithm for multi-baseline interferograms. *IEEE Trans Geosci Remote Sens*, 2015, 53: 494–504
- Xu W, Cumming I. A region-growing algorithm for InSAR phase unwrapping. *IEEE Trans Geosci Remote Sens*, 1999, 4: 124–134